Civil and Environmental Research
ISSN 2224-5790 (Paper) ISSN 2225-0514 (Online)
Vol.8, No.5, 2016

Improvement of Cracking Resistance for the Semi-Rigid Base Layer Reinforced by Geogrid

Zhu Yun Sheng* Chimi Tegachouang Nathan
School of Transportation, Wuhan University of Technology, # 205 Luoshi Road, Wuhan, P.R

Abstract
Reinforcement using an interlayer system appears nowadays as one of the techniques which is commonly used in asphalt pavement construction to improve its performances, extend its projected service life and reduce its structural cross section. Among a large number of existing interlayer systems, the geogrid has shown an effective use in pavement reinforcement with hot mix asphalt overlay. This article aims to research the mechanism leading to the spread of reflective crack and the anti-cracking effect of geogrid in semi-rigid pavement. The 3D finite element modeling package (ANSYS) has been used as tool to analyze the mechanical response of pavement model unreinforced and reinforced with different numbers of geogrid placed at different positions in the base layer under the influence of axle load. The results obtained from the finite element analysis have shown that, the use of geogrid in the semi-rigid base aids to reduce the stresses and strains both at the bottom of asphalt and base layer.
Keywords: Reinforcement, Asphalt pavement, geogrid, Reflective crack, Anti-cracking effect.

1. Introduction

Semi-rigid pavement is generally defined as a pavement section having some type of chemical stabilized layer as base layer (Cement treated base) below the HMA layer. This type of pavement is widely used in road construction worldwide and it has become the pavement structure of high-grade highway in China. However under the effects of traffic load and environmental factors, the pavement gradually suffers from damages which reduce its functional performances. One of the serious damages associated to the semi-rigid pavement is ‘’the phenomenon of reflective cracking’’.

Cracks from existing pavement that come up through a new surface or overlay is called reflective cracking. The development of this cracks consists of the following phases: phase 1: crack initiation triggered by the presence or appearance of default or a discontinuity in the underlying layer, the speed of this phase is function of the stresses concentration, the behavior of lower layer and that of the interface., phase 2: propagation in upper layer, which depends on the load, the thickness and rigidity of asphalt), and phase 3: breaking of asphalt surface layer.

The primary mechanisms behind reflective cracking are horizontal and vertical movements in the underlying old pavement at the vicinity of joint or cracks (Bozkurt 2002). Reflective cracks are differentiated according to their shape, configuration and the cracking mode (type I.II or III [Lee et al. (2007)]). Vehicle wheel loads approaching a crack in the underlying layer creates both vertical differential displacements which generate from a fracture mechanics point of view, the cracking Mode II (in plane shearing), and horizontal movement, Mode I (opening mode I). In addition the temperature changing between day and night and also between the summer and winter may cause a cracking Mode I opening mode I). Finally, Mode III (tearing mode) cracking sometimes occurs when the vehicle travels alongside a longitudinal crack.

Several empirical, mechanistic, and mechanistic-empirical (M-E) design methods of pavement have been proposed in order to solve the problem of reflective cracks. While empirical design approach is based solely on the results of experiments or experience, the mechanistic design approach is based on the theories of mechanics to relate pavement structural behavior and performance to traffic loading and environmental influences. Mechanistic-empirical (M-E) design combines features from both the mechanistic and empirical approaches. Lytton et al.1993 presented a mechanistic design method that uses theory to predict stress, strain and distress for pavements. Eltahan and Lytton 2000) presented an M-E design approach against reflective cracking, based on an integration of Paris’ law for estimating the number of Equivalent Single Axle Loads (ESAL) for crack propagation.

Various treatments techniques have been proposed in order to mitigate (delaying) reflective cracking through the AC overlay. For example before placing the overlay on the existing PCC, it is important to repair, clean, level and coat it with a binding agent (WSDOT 2009, TxDOT 2009).These techniques help insure the bonding of the overlay to the existing surface. It is also recommended to provide a sufficient thick of AC on the PPC pavement. FHWA based on performance survey found that breaking/cracking and seating (B/C&S) as a rehabilitation alternative should be approached with caution, as a significant reduction in reflective cracking after 4 to 5 years due to B/C&S occurred on only 2 of 22 projects reviewed (Galal et al. 1999, Thompson 1989). The use of Interlayer, Grids and Fabrics helps to absorb joint movement, delay reflective cracking and protect the existing underlying concrete pavement Blankenship et al. (2004). Button and Lytton (2007) observed that current

treatment strategies only delay the occurrence and do not prevent the development of reflective cracking.

1.1 Research aim

The aim of this paper is to assess the effectiveness of using geogrid in order to mitigate the propagation of reflective cracks in semi-rigid asphalt pavements.

1.2 Research objectives

The parameters being studied include:

- The mechanical response of pavement reinforced with geogrid (s);
- The influence of the number of geogrid and their location on the mechanical response of asphalt pavement structure

2 Finite Element modeling of asphalt pavement.

2.1 Model Geometry

Three - dimensional FE model was performed for developing the proposed model. ANSYS 14.5 software was used as a finite element tool for building and analyzing the model. The model of pavement proposed in this research is composed of three layers asphaltic concrete, base layer, subbase, and a subgrade layer. The dimensions of the pavement section considered are: 5000 mm along the length of the pavement, 5000mm along of the width and the total depth of the pavement is 10710 mm. The following elements types from ANSYS software were used for modeling the pavement and geogrids:

- All the pavement layers were modeled by using 8 nodes solid elements (SOLID45). This element is defined by 8 nodes having three degrees of freedom at each node, translations in x, y, and z direction at each node. (Figure 13) shows the geometry of element Solid 45.
- Geogrid was modeled by elements SHELL 63, which has both bending and membrane capabilities. The element has six degrees of freedom at each node: translations in the nodal x, y, and z directions and rotations about the nodal x, y, and z-axes. Stress stiffening and large deflection capabilities are included. Figure1 shows the geometry of element SHELL 63.

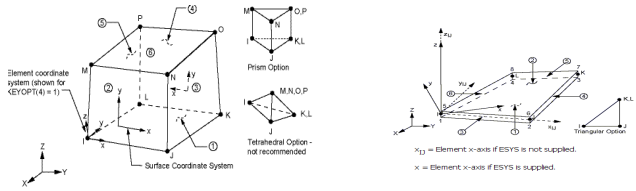

SOLID 45 Geometry SHELL 61 Geometry

Figure1: SOLID 45 and SHELL 61 Geometry (source ANSYS)

2.2 Structure of Pavement with Geogrids

The pavement was reinforced in different cases of reinforcement with one, two, three layers of geogrid. For each case of reinforcement, different positions of geogrids within the pavement structure have been taken into account. Figure 2 shows the position of geogrids in different cases of reinforcement.

- 1st case of reinforcement: pavement is reinforced by 1 layer of geogrid.

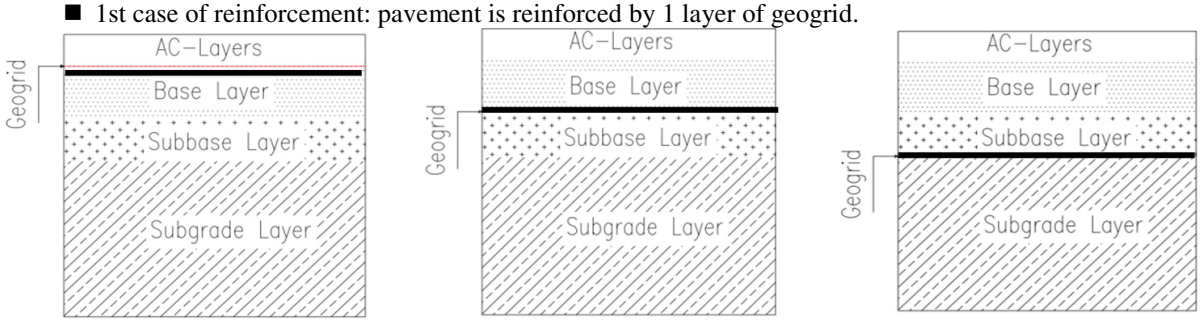

1-a 1-b 1-c

■ 2nd case of reinforcement: pavement is reinforced by two layers of geogrid.

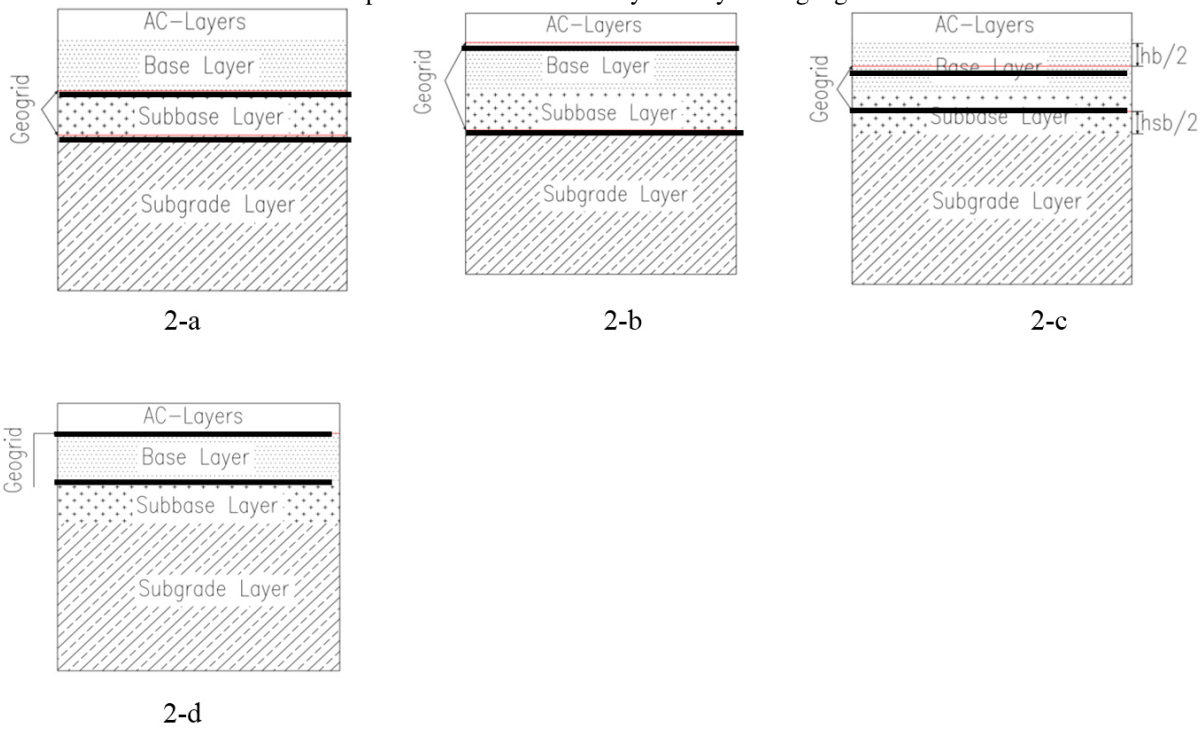

2-a 2-b 2-c

2-d

■ 3rd case of reinforcement: pavement is reinforced by 3 layers of geogrid.

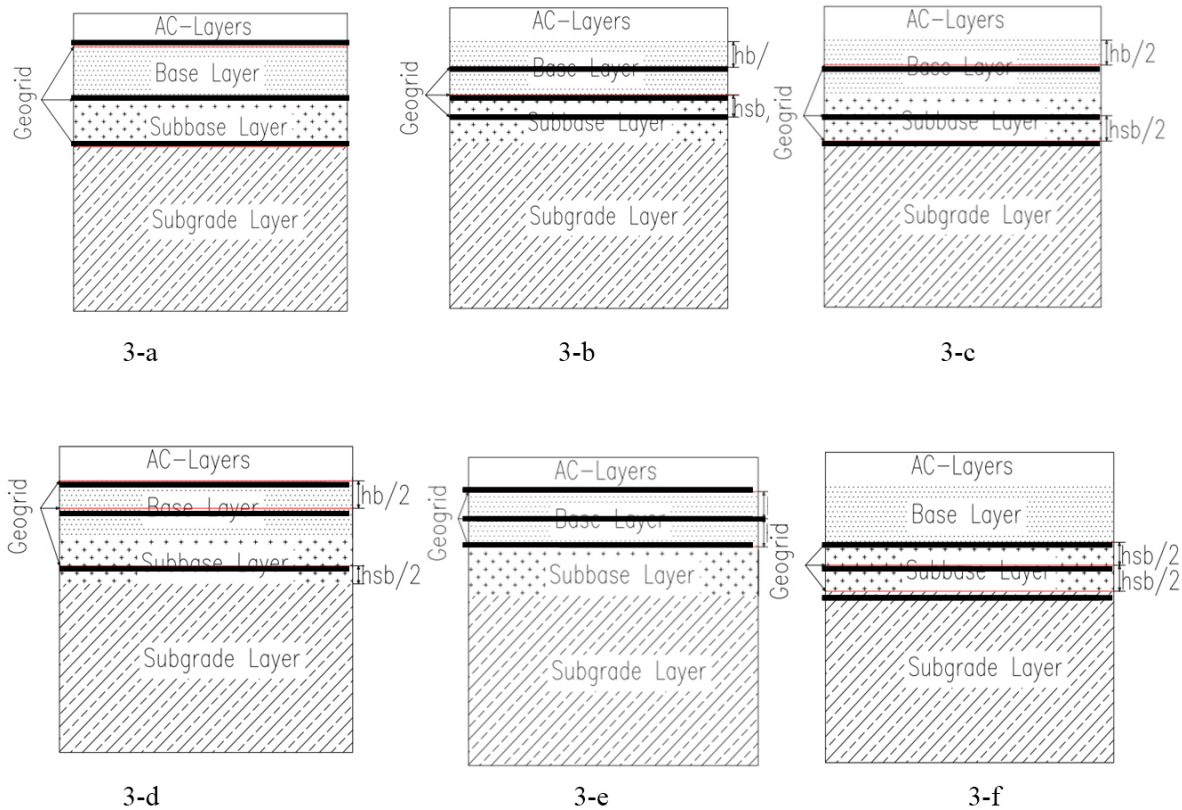

3-a 3-b 3-c

3-d 3-e 3-f

Figure2: Geogrid location in parametric study (hb= thickness of the base layer and hsb= thickness of the subbase).

2.3 Material Properties

Pavement materials and geogrid in the FE models were assumed to be linear elastic although the pavement may exhibit nonlinear elastic behavior. To perform the analysis, the following assumptions have been made:

- The structure of the pavement is composed of a 6-layers system;
- Each layer is homogeneous, isotropic, and linear elastic;
- Properties of each layer are characterized by a permanent elastic modulus E and a Poisson's ratio v;
- Each layer has a finite thickness h, even the subgrade layer, for a better control of the model;
- Continuity condition are satisfied at the layer interfaces, as indicated by the same vertical stress, shear stress, vertical displacement, and radial displacement.

The materials properties of each layer of the pavement and the geogrid are recapitulated in the following tables

Table1: Material properties of pavement structure in the FE model.

Layer No.	Material	Depth (mm)	Elastic Modulus (MPA)	Poisson's Ratio(v)
1	Asphalt Mix layer (AC-16)	50	1400	0.3
2	Asphalt Mix layer (AC-20)	60	1200	0.3
3	Asphalt Mix layer (AC-25)	70	1000	0.3
4	Cement stabilized gravel base	330	1500	0.20
5	Cement stabilized subbase soil	200	1300	0.25
6	Subgrade	10000	60	0.45

Table2: Material properties of geogrid in the FE model.

Parameters of Geogrid	
Thickness (m)	0.00254
Modulus of elasticity (MPA)	4230
Poisson ration	0.35

2.4 Interface model

Due to the fact that the pavement structure is composed of a multilayers system, the interface between different layers of material should be take into account while their FE modeling. For the modeling of pavement-reinforced the following assumptions were made:

- Full bonding between all the layers of the pavement structure;
- Full bonding in the two contact interfaces between geogrid element and pavement layer(s)

2.5 Meshing of the model

The 3D model of the pavement structure is meshed finely close to the load area. The regions farther away from the loading area isn't critical like the region close to the loading region. Therefore the mesh in these regions were realized a bit coarser, in order that the analysis be faster.

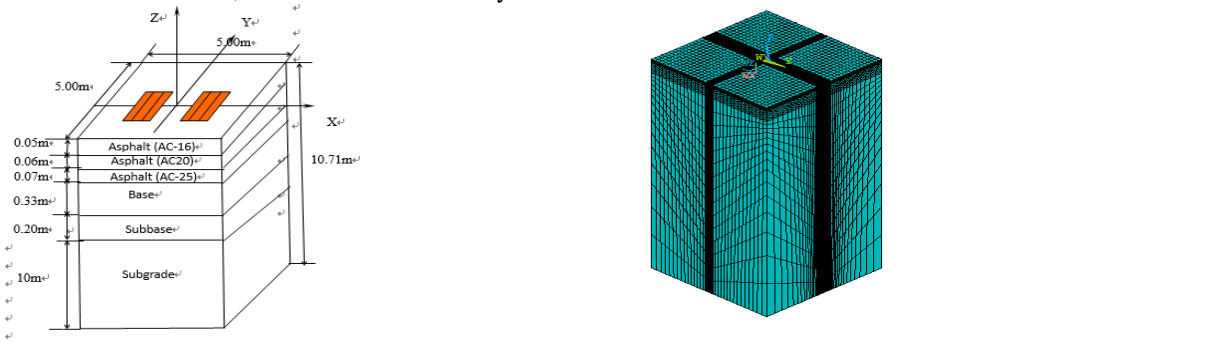

Figure 3: FE model mesh of pavement structure.

2.6 Boundary conditions

- Boundary condition at the edges parallel to traffic direction (parallel to Y-axis)

The horizontal displacement of the nodes in x-direction is fixed (Ux=0).

- Boundary condition at the edges perpendicular to traffic direction (parallel to X-axis)

The horizontal displacement of the nodes in y-direction is fixed (Uy=0).

- Boundary condition at the bottom Plane of the Model

The vertical displacement (along z-direction) of the nodes on the bottom plane of the model are fixed.

- Boundary condition at the edges of geogrids (especially for pavement reinforced).

The horizontal displacement of the nodes at the edges of geogrids are fixed.
There is no boundary condition at the top of the asphalt surface layer (i.e. the surface on which the static load is applied).

2.7 Modeling of loads applied on Pavement.

For conventional flexible pavement analysis, the layered elastic theory is commonly used; tire loading is assumed as uniform tire-pavement contact stresses (equal to tire inflation pressure) applied through a stationary circular contact area. Unfortunately, these assumptions are inconsistent with realistic loading conditions and may result in erroneous pavement response calculation and pavement damage prediction Al-Qadi et al. (2008). In this study in order to be close to the reality, we assumed that the contact shape between the pavement surface and the wheel is rectangular, and the wheels pressure is not uniformly distributed in all the contacting area. The following picture show the contact shape of the wheel on the pavement surface.

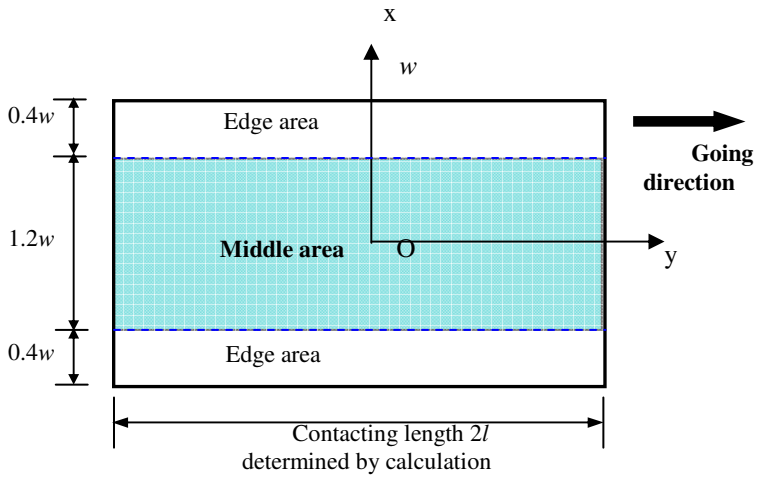

Figure 4: sketch of contacting pressure area of wheel load.

The wheel is divided into three regions: 20%, 20% of the wheel width respectively for each edge area. The vertical contacting pressure of middle area and edge area is expressed in the following regression equations according to the Chinese standard:

$$q_{zc} = a_0 + a_1 \cdot p_i + a_2 \cdot P_z \quad (1)$$

$$q_{ze} = b_0 + b_1 \cdot p_i + b_2 \cdot P_z \quad (2)$$

Where： q_{Zc} vertical contacting pressure of middle area, KPa；

q_{Ze} vertical contacting pressure of edge area，KPa；

p_i inner pressure of tire，KPa；

P_Z vertical wheel loading, KN；

a_i, b_i regression coefficient，see table 1

Table 3: regression coefficient

coefficient / type of tire	Middle area $q_c(kPa)$ parameter			Edge area $q_e(kPa)$ parameter		
	$a_0(kPa)$	a_1	a_2	$b_0(kPa)$	b_1	b_2
diagonal tire	-15.588	0.541	4.179	379.532	0.026	4.629
Radial ply tyre	190.230	0.438	0.864	185.205	0.046	10.789

Because:

$$q_{zc} \cdot (1.2w \times 2l) + q_{ze} \cdot (0.8w \times 2l) = P_z \quad (3)$$

So, the contacting length between tire and pavement is:

$$l = \frac{5 \cdot P_z}{4w \cdot [(3a_0 + 2b_0) + (3a_1 + 2b_1) \cdot p_i + (3a_2 + 2b_2) \cdot P_z]} \quad (4)$$

Where： l half of contacting length, m;

w Half of contacting area width between tire and pavement, cm

Table 4 below gives the axle load, the tire size and the tire pressure that have been taking into account in this study.

Table 4: wheel load and tire ground size calculation results.

Axle load (KN)	100
Wheel Load（KN）	50
Tire pressure（Mpa）	0.75
Center wheel pressure（Mpa）	0.60
Edges pressure（Mpa）	0.63
Width of rectangle（cm）	26.3
Length of rectangular（cm）	31.1

In accordance with the standard model to calculate the area of a ground wheel load, tire width is 26.3cm, wheel center spacing of 34.6cm. The selector wheel clearance center A, the inner edge of the wheel track point B, the wheel track center C, the outer edge of the wheel track point D are the four calculation points location see Figure 5

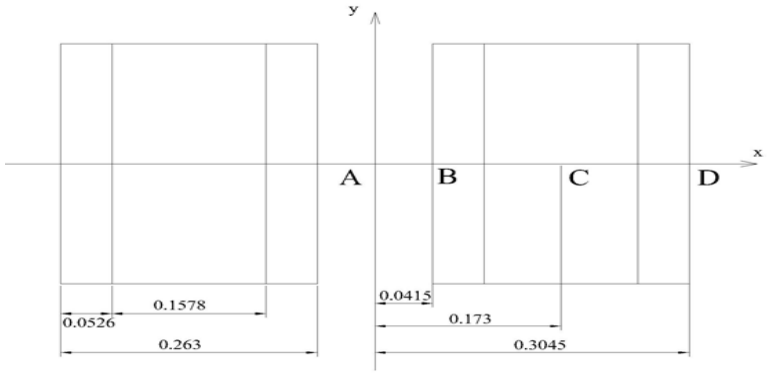

Figure 5: Position of points chosen for computation of stresses and strains in the pavement structure.

3 Results of finite element analysis

In the following sections, the analytical discussions of the results of the finite element analysis are presented

3.1 Shear strain

Figures 6, 7 and 8 show respectively the horizontal shear strain at the bottom of the asphalt layers (U_Z=-0.18m) when the pavement is unreinforced and reinforced with one, two and three layers of geogrid put at different positions. It is noted from these figures that the inclusion of the geogrid layer resulted in significant reduction of the shear strain at the bottom of asphalt layers.

Figure 6 shows that, the reinforcing effect is more important when the geogrid layer is put at the top of the base or else at the interface between the base and the asphalt layers. The maximum shear strain at the bottom of asphalt layers is $2.45x10^{-4}$ in pavement model unreinforced and it is located at -0.16m and 0.16m, on either side of the center of dual wheel. When the pavement is reinforced with one layer of geogrid placed at the top of base course, the shear strain decreases from $2.45x10^{-4}$ to $2.25x10^{-4}$ i.e. 8% of reduction.

Figure 7 illustrates that when the pavement is reinforced with two layers of geogrid, the effect of reinforcing is more significant when one layer of geogrid is put respectively at the top of the base and the top of the subbase. The maximum shear strain decreases from $2.45x10^{-4}$ to $2.14x10^{-4}$ i.e. 13% of reduction.

Figure 8 shows that when the pavement is reinforced with three layers of geogrids, the reinforcing effect is more considerable when one layer of geogrid is respectively put at the top, middle and the bottom of the base course. The maximum shear strain decreases from 2.45x10-4 to 2.06x10-4 i.e. 16% of reduction.

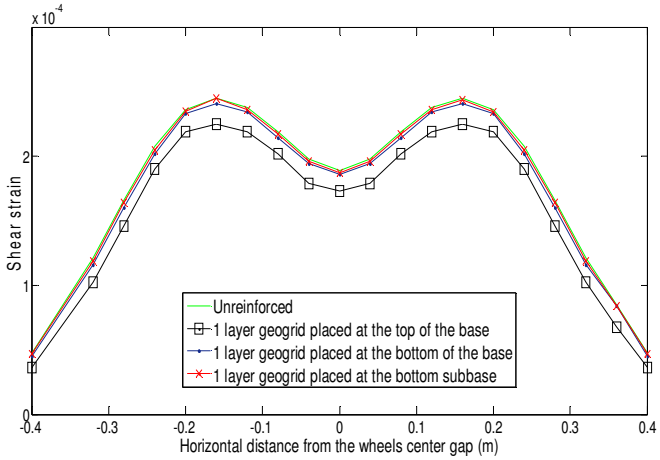

Figure 6: Horizontal shear strain at the bottom of asphalt layers when pavement is unreinforced and reinforced with one layer of geogrid placed at different positions

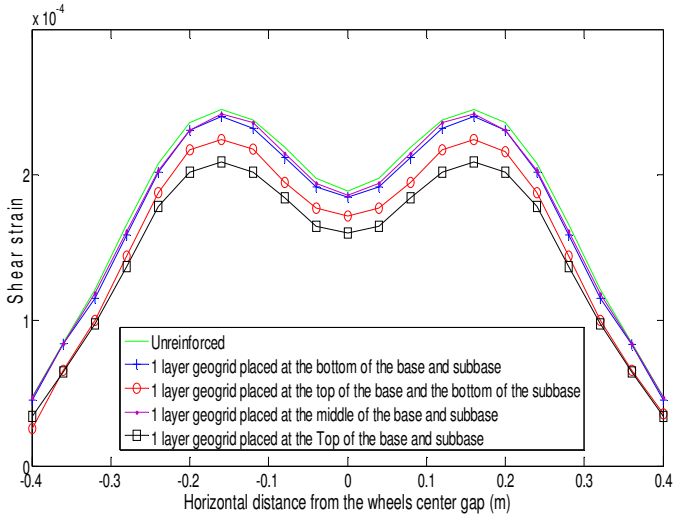

Figure 7: Horizontal shear strain at the bottom of asphalt layers when pavement is unreinforced and reinforced with two layers of geogrid placed at different positions

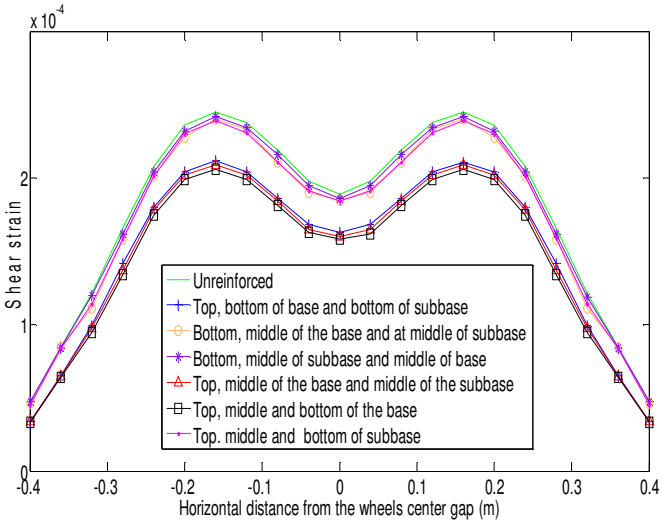

Figure 8: Horizontal shear strain at the bottom of asphalt layers when the pavement is unreinforced and reinforced with three layers of geogrid placed at different positions.

3.2 Tensile stress

Figures 9, 10 and 11 show respectively the horizontal tensile stress distribution at the bottom of base layer (U_Z=-

0.51m) when the pavement is unreinforced and reinforced with one, two and three layers of geogrid put at different positions. It is noticed from these figures that the use of geogrid helps to reduce the tensile stress at the bottom of the base layer.

Figure 9 illustrates that when the pavement is reinforced with one layer of geogrid, the reduction is more significant when the geogrid is put at the top of the base course. The maximum tensile stress at the bottom of the base layer decreases from $7.27x10^4$ Pa to $5.19x10^4$ Pa, i.e.29% of reduction.

Figure 10 shows that when the pavement is reinforced with two layers of geogrids, the reduction of the tensile stress is more considerable when one layer of geogrid is put respectively at the top of the base and the top of the subbase. The maximum tensile stress at the bottom of the base layer decreases from $7.27x10^4$ Pa to $5.01x10^4$ Pa, i.e.31% of reduction.

Figure 11 shows that when the pavement is reinforced with three layers of geogrids. The reduction of the tensile stress is more significant when one layer of geogrid is put respectively at the top. middle and bottom of the base course. The maximum tensile stress at the bottom of the base layer decreases from 7.27 $x10^4$ Pa to 4.79 $x10^4$ Pa, i.e. 34% of reduction.

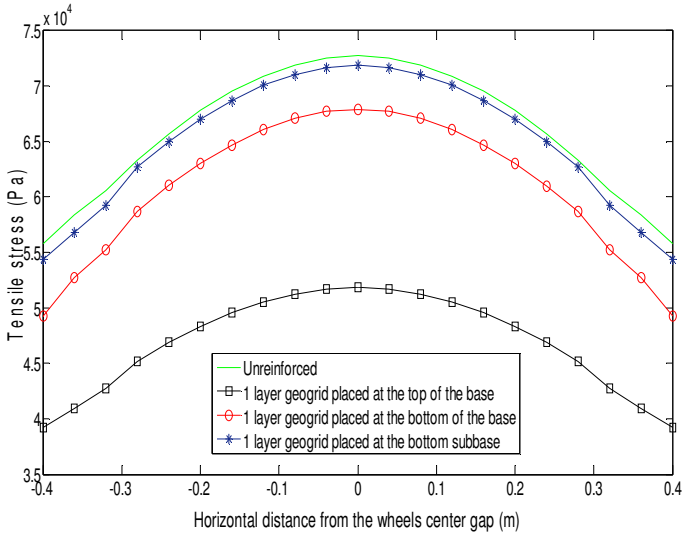

Figure 9: Horizontal tensile stress at the bottom of base layer (when pavement is reinforced with one layer geogrid placed at different positions)

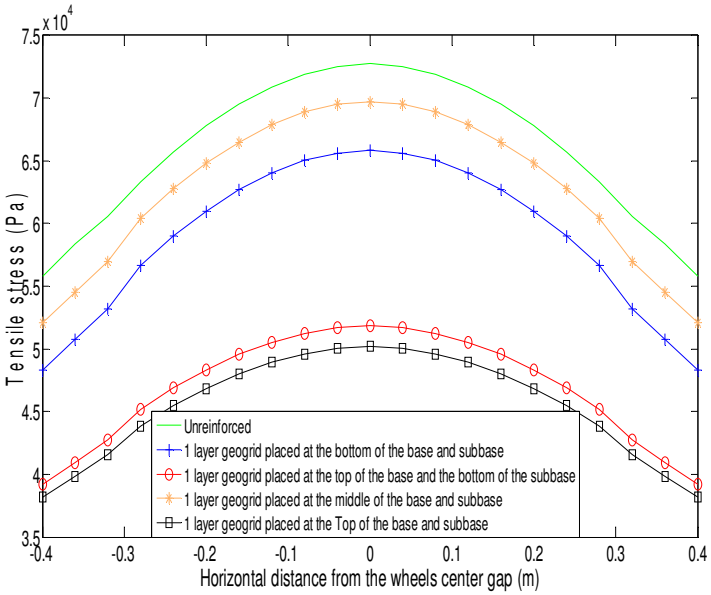

Figure 10: Horizontal tensile stress at the bottom of base layer (when pavement is reinforced with two layers geogrid placed at different positions)

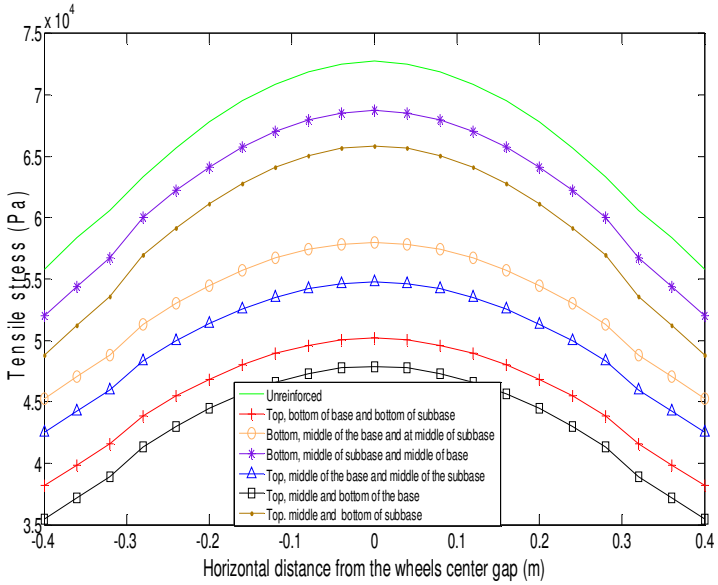

Figure 11: Horizontal tensile stress at the bottom of base layer (when pavement is reinforced with three layers geogrid placed at different positions)

3.3 Vertical strain

Figures 12, 13 and 14 show the Horizontal tensile strain at the bottom of asphalt layers when the pavement is unreinforced and reinforced with one, two and three layers of geogrid put at different positions. The figures clearly demonstrate that the geogrid layer helps to reduce the tensile strain at the bottom of asphalt layers.

Figure 12 shows that when the pavement is reinforced with one layer of geogrid, the reduction is more significant when the geogrid is put at the top of the base or else at the interface between the base and the asphalt layers. The inclusion of geogrid at the top of the base can reduce up to 20% of the vertical strain within the asphalt layers.

Figure 13 illustrates that when the pavement is reinforced with two layer of geogrid, the reduction is more important when one layer of geogrid is put respectively at the top of the base and the top of subbase. The reduction of the tensile strain within the asphalt layers can reach up to 24%.

Figure 14 shows that when the pavement is reinforced with three layers of geogrid, the effect of reinforcing of the tensile strain at the bottom of asphalt layers is more considerable when one layer of geogrid is put respectively top, middle and bottom of the base layer. The reduction of the tensile stress at the bottom of asphalt layer can reach up to 30%.

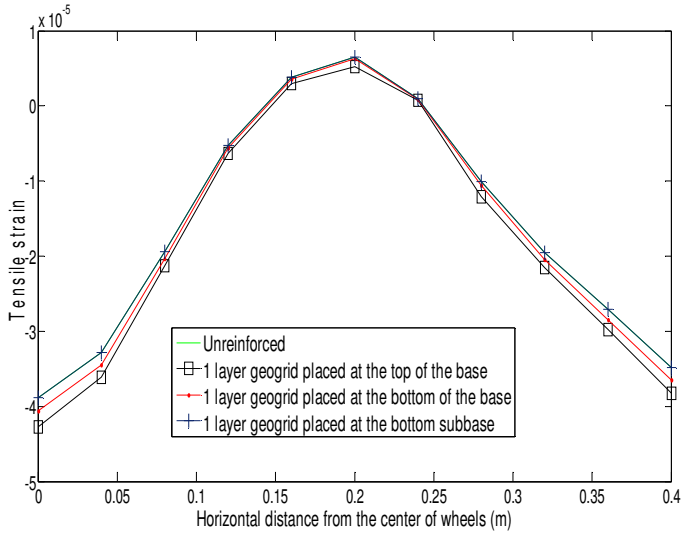

Figure 12: Horizontal tensile strain at the bottom of asphalt layers (when pavement is reinforced with one layer geogrid placed at different positions)

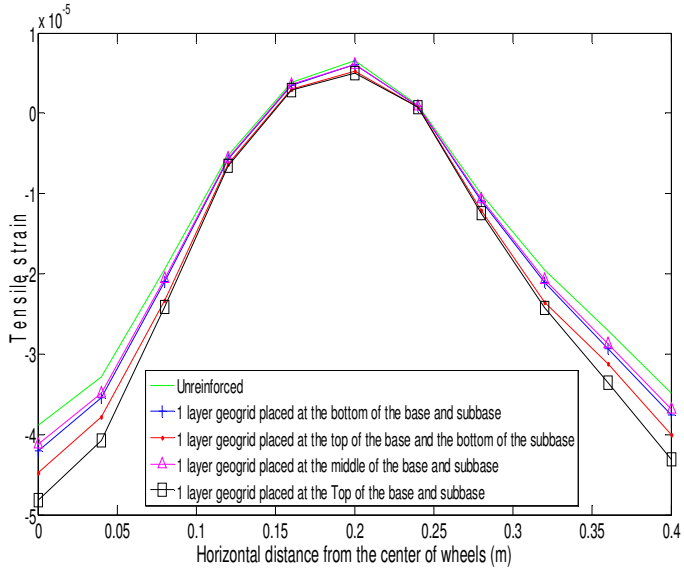

Figure 13: Horizontal tensile strain at the bottom of asphalt layers when pavement is unreinforced and reinforced with two layers of geogrid placed at different positions

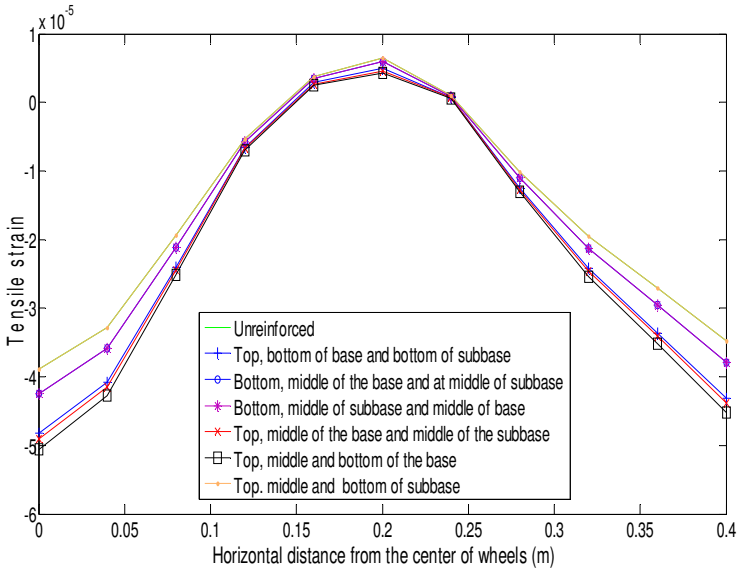

Figure 14: Horizontal Tensile strain at the bottom of asphalt layers when the pavement is unreinforced and reinforced with three layers of geogrid placed at different positions.

4. Conclusion

The following conclusions can be made from the study:

(i) The use of geogrid can be helpful to mitigate the propagation of reflective cracking in semi-rigid pavement. From the finite element analysis results, it has been found that just one layer of geogrid placed at the top of the base layer can aid to reduce up to 8% of the shear strain and 20% of tensile strain at the bottom of asphalt layers and also up to 29% of tensile stress at the bottom of the base layer.

(ii) The reinforcing efficiency does not depend only of the number of geogrid but also of the good position of geogrid layer(s) in the pavement. It has been found that, the reinforcing effect is most effective when the geogrid is placed at the top of base or at the interface between asphalt layers and base course.

5. Recommendation

In order to mitigate the reflective cracking in semi-rigid pavement, it is recommended to put the geogrid layer at the interface between asphalt layer and the base layer.

6. References

Bozkurt, D., “Three Dimensional Finite Element Analysis to Evaluate Reflective Cracking Potential in Asphalt

Concrete Overlays." Ph.D. Dissertation, Department of Civil and Environmental Engineering, University of Illinois at Urbana-Champaign, 2002.

Lee, S.W., Bae, J.M., Han, S.H., and Stoffels, S.M. 2007. "Evaluation of Optimum Rubblized Depth to Prevent Reflection Cracks." Journal of Transportation Engineering. ASCE, 133 (6): 355–361.

Lytton, R.L., Uzan, J., Fernando, E.G., Roque, R., Hiltunen, D., and S.M. Stoffels. (1993). Development and Validation of Permanent Prediction Models and Specifications for Asphalt Binders and Paving Mixes, SHRP Report A-357, Strategic Highway Research Program, National Research Council, Washington, D.C.

Eltahan, A. A. and Lytton, R. L. (2000). "Mechanistic-empirical approach for modeling reflection cracking," Transportation Research Record, No. 1730, pp. 132 – 138.

WSDOT http://training.ce.washington.edu/wsdot/modules/07_construction/07-2_body.htm accessed July 2009.

TxDOT http://onlinemanuals.txdot.gov/txdotmanuals/pdm/manual_notice.htm accessed July 2009.

Galal, K., Coree, B., Haddock, J., White, T. Structural Adequacy of Rubblized Portland Cement Concrete Pavement. Transportation Research Record 1684, TRB, National Research Council, Washington D. C, 1999.

Thompson, M. BREAKING/CRACKING AND SEATING CONCRETE PAVEMENTS. Transportation Research Board. NCHRP Synthesis of Highway Practice, No. 144, 1989.

Blankenship, P., Iker, N., and Drbohlav, J. (2004). "Interlayer and design considerations to retard reflective cracking," Transportation Research Record, No. 1896, pp. 177 – 186.

Button, J. W. and Lytton, R. L. (2007). "Guidelines for using geosynthetics with hot-mix asphalt overlays to reduce reflective cracking," Proceedings of the 86th Annual Meeting of the Transportation Research Board (CD-ROM), Washington, D.C.

Al-Qadi I.L., H. Wang, P.J. Yoo, and S.H. Dessouky (2008). Dynamic Analysis and Insitu Validation of Perpetual Pavement Response to Vehicular Loading, Transportation Research Record, 2087, p. 29-39.